AD-A156 291 EXPERIMENTAL INVESTIGATION OF CERTAIN BEAM TRANSPORT ISSUES IN A PULSED T..(U) SANDIA NATIONAL LABS ALBUQUERQUE NM M G MAZARAKIS ET AL. 1983 SAND84-0095 1/1

UNCLASSIFIED DE-AC04-76DP00789 F/G 20/7 NL

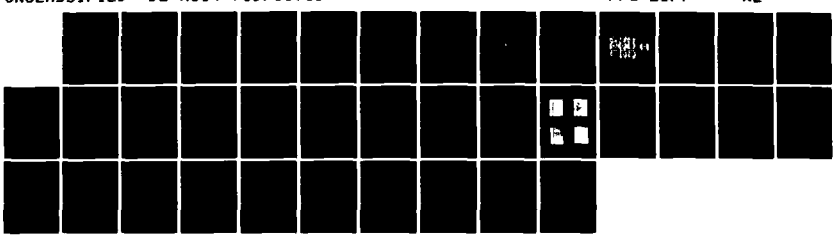

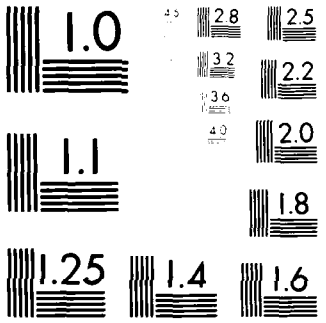

MICROCOPY RESOLUTION TEST CHART

SAND84-0095

EXPERIMENTAL INVESTIGATION OF CERTAIN BEAM TRANSPORT ISSUES IN A PULSED TRANSMISSION LINE LINEAR ACCELERATOR

M. G. Mazarakis, R. B. Miller, S. L. Shope,
L. E. Stevenson, D. P. Coleman, J. W. Poukey,
Sandia National Laboratories, Albuquerque, NM 87185

R. J. Adler
Mission Research Corporation

T. C. Genoni
U.S.M.A. West Point

ABSTRACT

The successful development of a new generation of high current, high voltage, linear induction accelerators relies on the solution of a number of beam transport problems, including radial oscillations, diocotron instabilities, transverse beam break-up (BBU), etc.

Most of the instabilities appear to onset either at the injector region or at the accelerating gaps. Radial oscillations were first observed in RADLAC I, while transverse beam break-up was first observed on the SLAC accelerator, and more recently on the ETA accelerator.

A low emittance, high current, high voltage injector precisely aligned with the guiding magnetic field axis and beam vacuum pipe axis is of prime importance for successful beam acceleration and transport. Similarly, an accelerating gap design which maintains radial force balance and an accelerating cavity with low Q and very small transverse shunt impedance $Z_\perp$ should eliminate the most dangerous radial oscillations and beam break-up instabilities.

TABLE OF CONTENTS

The design and experimental studies of a new 4 MeV, 40 kA electron beam injector and accelerating gap will be presented. Test bench measurements of $Z_\perp$ and Q on a typical radial transmission line accelerating cavity prove that BBU is not of concern unless the number of accelerating gaps become excessively large.

I. Introduction

In the last ten years, considerable work has been devoted to the production and acceleration of intense relativistic electron beams using linear induction accelerators.[1,4] Because of the extremely high currents involved, 10-100 kA, and the relatively large number of modules required, these accelerating structures are susceptible to a number of instabilities. Among the most dangerous are radial[4] oscillations and transverse beam break-up (BBU).[5] Radial oscillations can appear in the injector and the accelerating gaps and are mainly due to the lack of radial force balance in those regions. Transverse beam break-up is due to the excitation by the beam pulse of transverse electromagnetic modes in the accelerating cavities.

The analysis and means of avoiding these instabilities were the objectives of extensive analytical and numerical studies reported previously.[6,7] In this paper, we report the experimental work which also addressed the above instabilities. Section I describes the design and performance of a new 4 MeV, 40 kA foilless diode injector with low emittance and no radial oscillations. Section II involves the radial oscillation measurements on a new accelerating gap design with radial force balance. Finally, in

Section III, the test bench measurements of $Z_\perp$ and Q of typical pulsed transmission line cavity are presented and their significance in exciting transverse beam break-up modes is discussed.

II. IBEX Foilless Diode Injector

A new high voltage isolated Blumlein accelerator (IBEX) was designed and constructed for these injector experiments.[8] The isolated Blumlein is a new pulse-forming-line configuration whose greatest merit is the complete elimination of the familiar and troublesome prepulse of the conventional Blumlein geometry. The mechanism of pulse generation is inductive and at all times the anode and cathode electrode are at ground electrostatic potential. The IBEX accelerator fitted with a foilless diode source has become one of the most reliable intense electron beam injectors.[9,10] It is ideally suited for high current linear accelerators and, in particular, those utilizing solenoidal magnetic fields for beam focusing and transport. With the anode and cathode immersed in the same solenoidal field, the electron beam is directly created inside the guiding field of the accelerator.

IBEX can provide a maximum pulse of 4 MV, 100 kA and 20 ns FWHM when matched with a diode impedance equal to its characteristic 40 ohm impedance. The design goals for these experiments were 20-40 kA at 4 MV; hence, a higher impedance foilless diode was adopted. A schematic diagram of the foilless diode used with the relevant dimensions is shown in Fig. 1. Several annular cathode tips were used with different radii (r_c) and thicknesses (α). The axial anode-cathode gap could be varied in steps of 0.6 cm. The magnetic field was provided by an array

IBEX FOILESS DIODE PARAMETERS

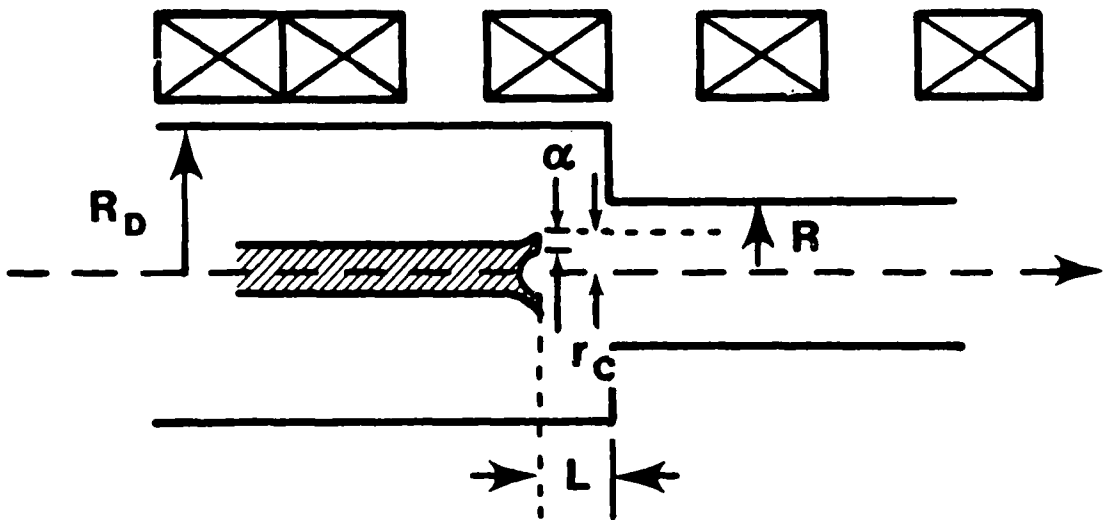

$16 \geqslant B_Z \geqslant 6$ kG
R = 2.9 cm
r_C = 1.3 cm (variable)
α = 2 mm (variable)
L = 3.2 cm (variable)
R_D = 7.3 cm

V_D = 4 MV
I_B = 20-30 kA
Z_D = 95-130 Ω
Z_L = 195 Ω

Figure 1. Schematic diagram of IBEX foilless diode injector.

of "pancake" coils connected in series to a capacitor bank. The peak magnetic field could be varied from 6 to 16 kG. Figure 2 is a schematic diagram of the experimental set-up including the foilless diode and vacuum transport line. Typical voltage and current waveforms are shown in Fig. 3. The beam propagates a distance of 10 cyclotron wavelengths in vacuum along a uniform magnetic field. Rogowski current monitors are positioned along the beam path to follow the beam current in a nondestructive way.

A systematic study of the diode performance and beam vacuum propagation was undertaken. The free variables of the experiments were anode-cathode voltage, axial magnetic field, cathode shank radius and anode cathode spacing. In all cases, we produced an excellent low emittance thin annular beam with practically no radial oscillations. Our concern with precisely aligning the diode axis with the magnetic field axis as well as the vacuum pipe axis gave the anticipated results.

Figure 4 shows the beam damage pattern on a set of brass witness plates for the radial oscillation measurements. The targets scanned an entire cyclotron wavelength distance and were positioned 1 cm apart for 9 consecutive shots. The magnetic field strength was 7 kG. We intentionally chose the lowest field because if there were radial oscillations they should appear most pronounced here. Figure 5 shows the measured beam outer diameter ($2r_b$) at various distances from the cathode. The points lie on a straight line indicating no radial oscillations. The vacuum beam transmission to the end of the drift pipe was 100%. No diocotron instabilities were observed.

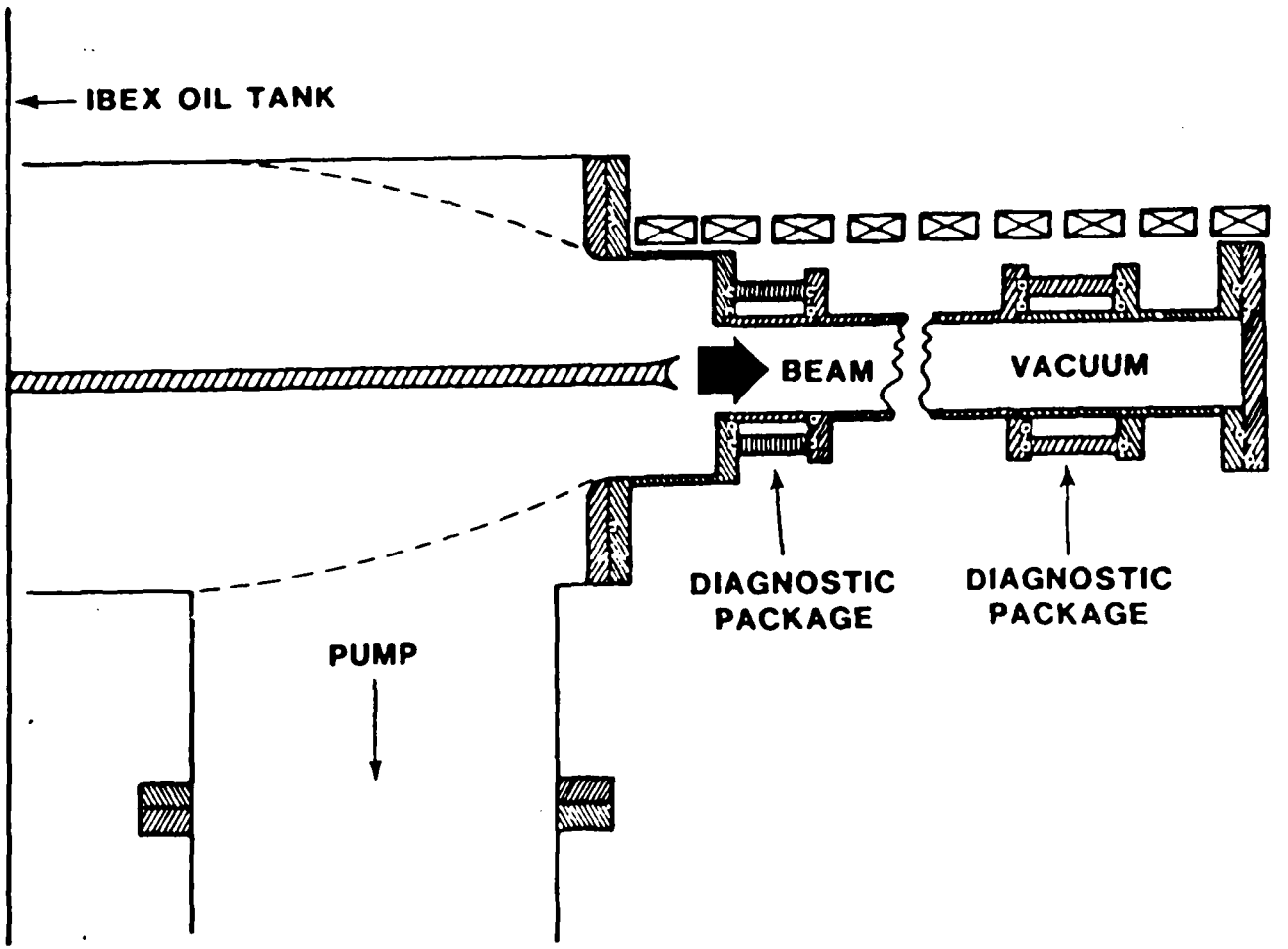

Figure 2. Diagram of the IBEX experimental setup including the diode and the vacuum transport line.

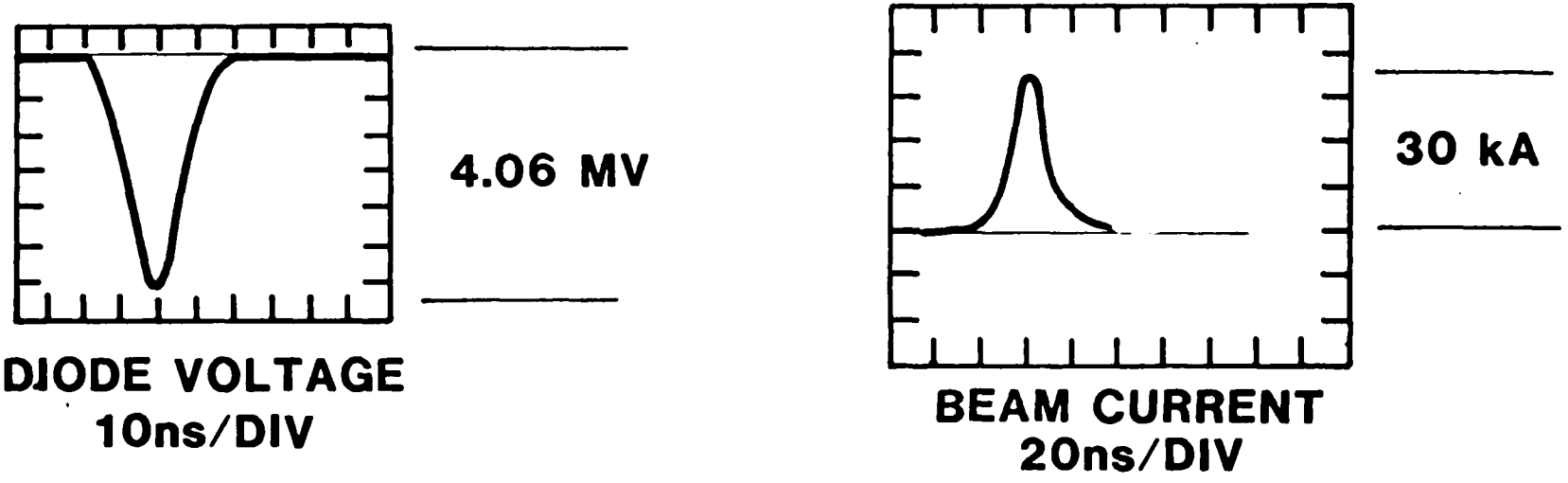

Figure 3. Typical foilless diode voltage and current waveforms.

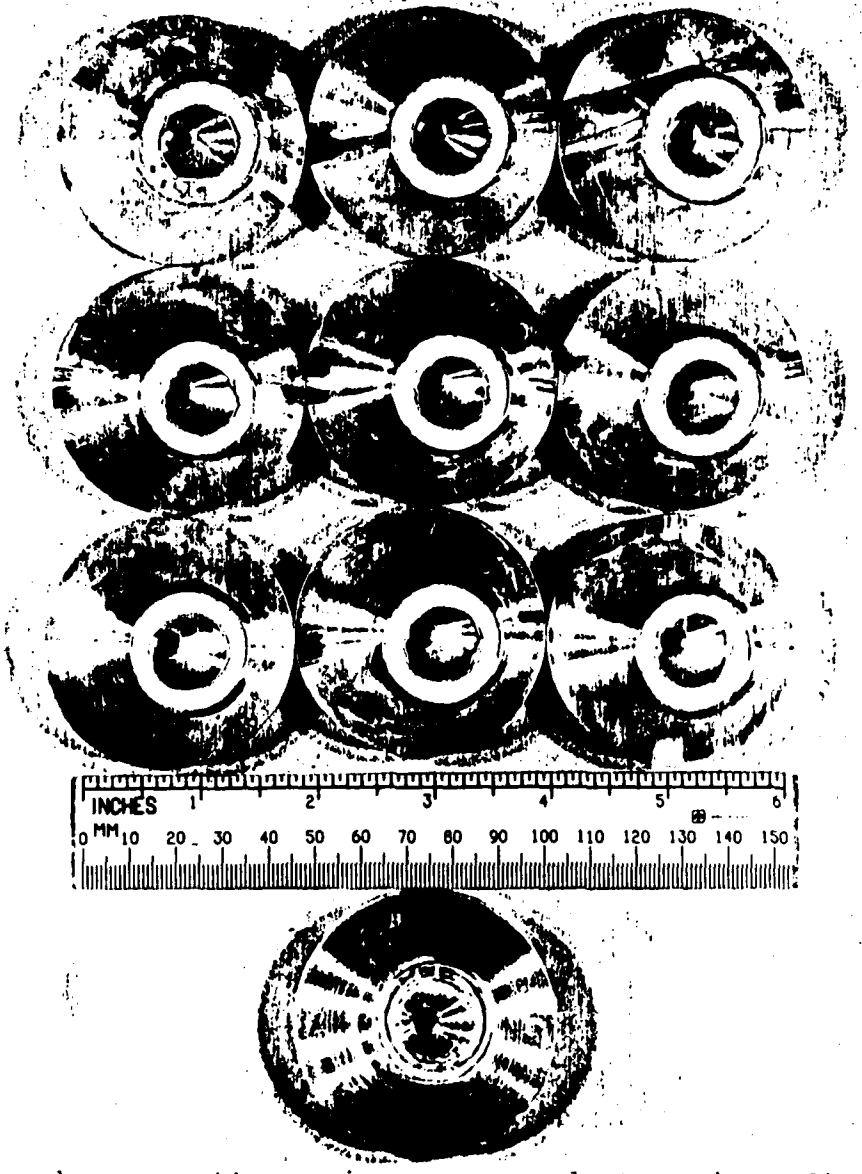

Figure 4. Beam damage patterns in vacuum and at various distances from the cathode for radial oscillations measurements. The nine targets above the ruler were obtained with 7 kG guiding field. The lower one was obtained with 14 kG. Some fine structure is observed in the 14 kG target.

At higher magnetic field strengths (~ 14 kG), a very fine structure composed of 30 to 40 filaments symmetrically located inside the beam annulus was visible on the witness targets (Fig. 4). This is mainly due to nonuniform cathode ignition and not to diocotron instability.

Figure 6 summarizes the results of our diode parametric study and shows that the most important variable for the range of B_z used is the anode-cathode spacing. In Fig. 7, the experimentally measured larmor radii appear to decrease quadratically with the field strength in agreement with the theory.[11] During the investigation, we fired the injector 200 times; the reproducibility of the beam parameters and the beam quality was very good.

III. Radial Oscillation Measurements of a Radial Force Balanced Accelerating Gap

One of the most important problems in the development of high current electron linear accelerators is the suppression of radial oscillations of the beam in the accelerating gaps. The oscillations arise because of the lack of radial force balance in the gap region and can cause deterioration of beam quality and severe beam losses. Several methods of suppressing radial oscillations were proposed and theoretically studied,[7,12] including contouring the magnetic field in the gap region and increasing the wall radius after each gap. These techniques are fairly easy to implement and require minor hardware modifications of the available RADLAC I accelerating gap structure. For these experiments the accelerating assembly was composed of the injector and one post accelerating gap. Figure 8 gives an outline of the

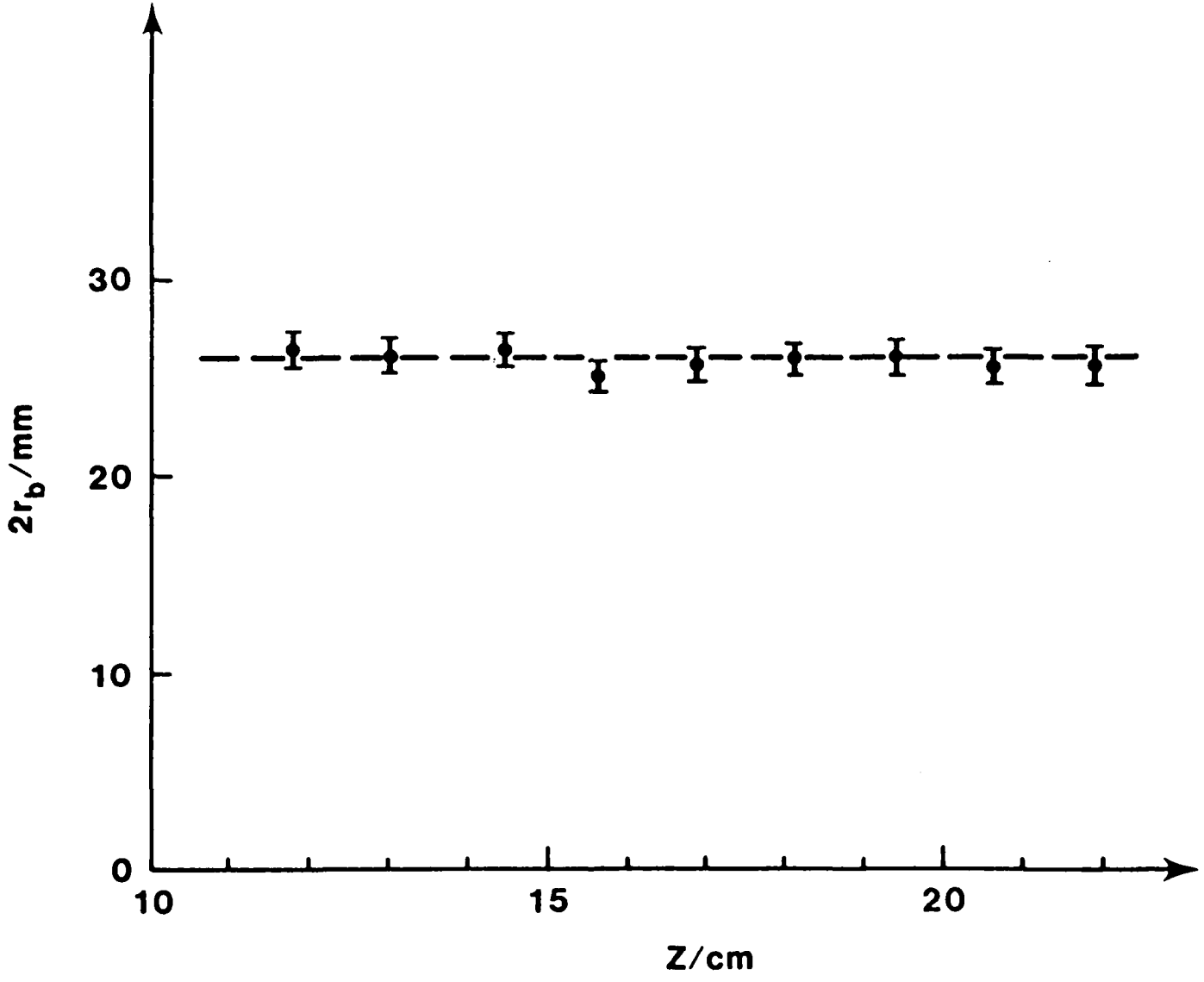

Figure 5. Axial variation of the beam envelope. The distance z of each measurement point is from the cathode plane.

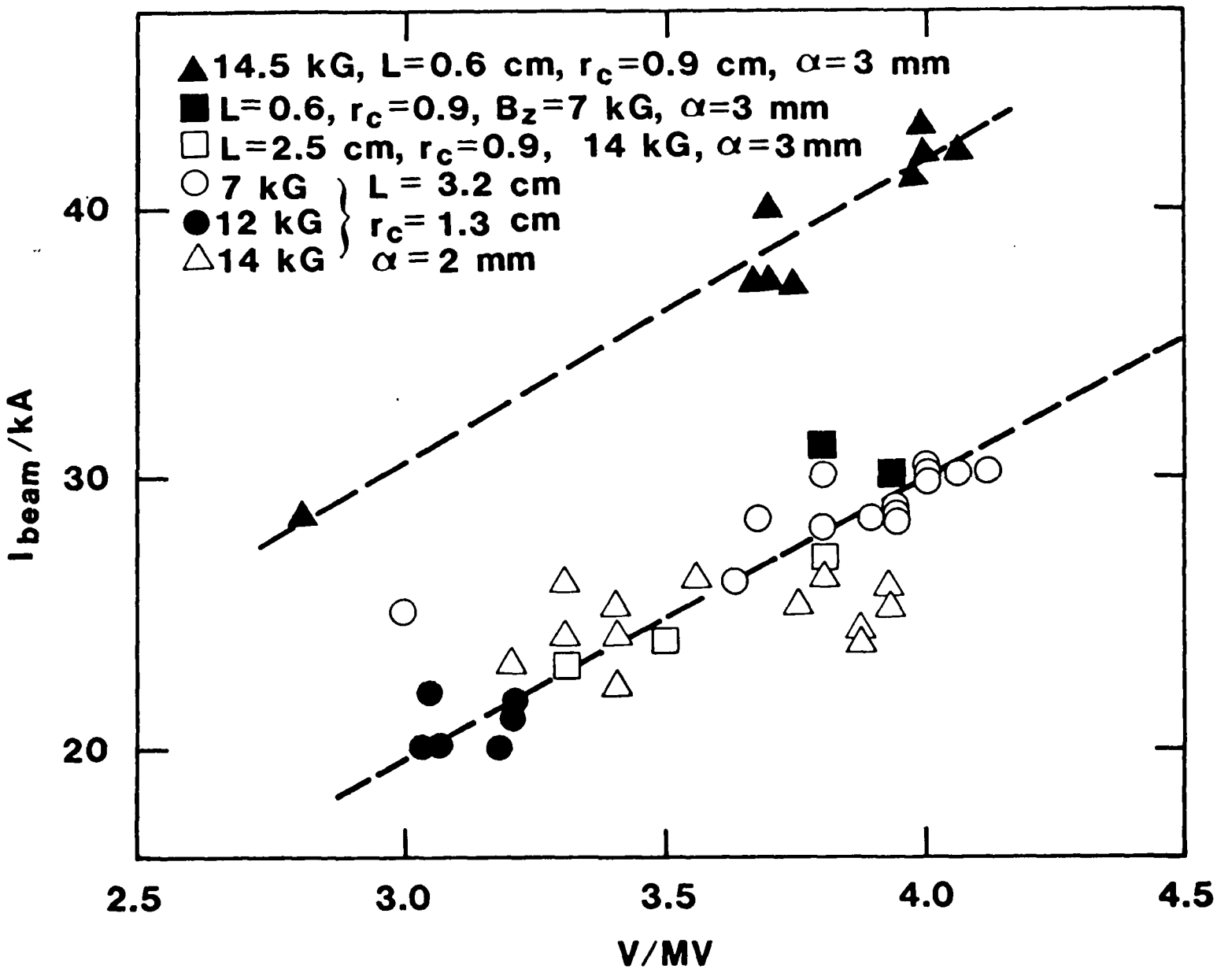

Figure 6. Measured beam current versus diode voltage.

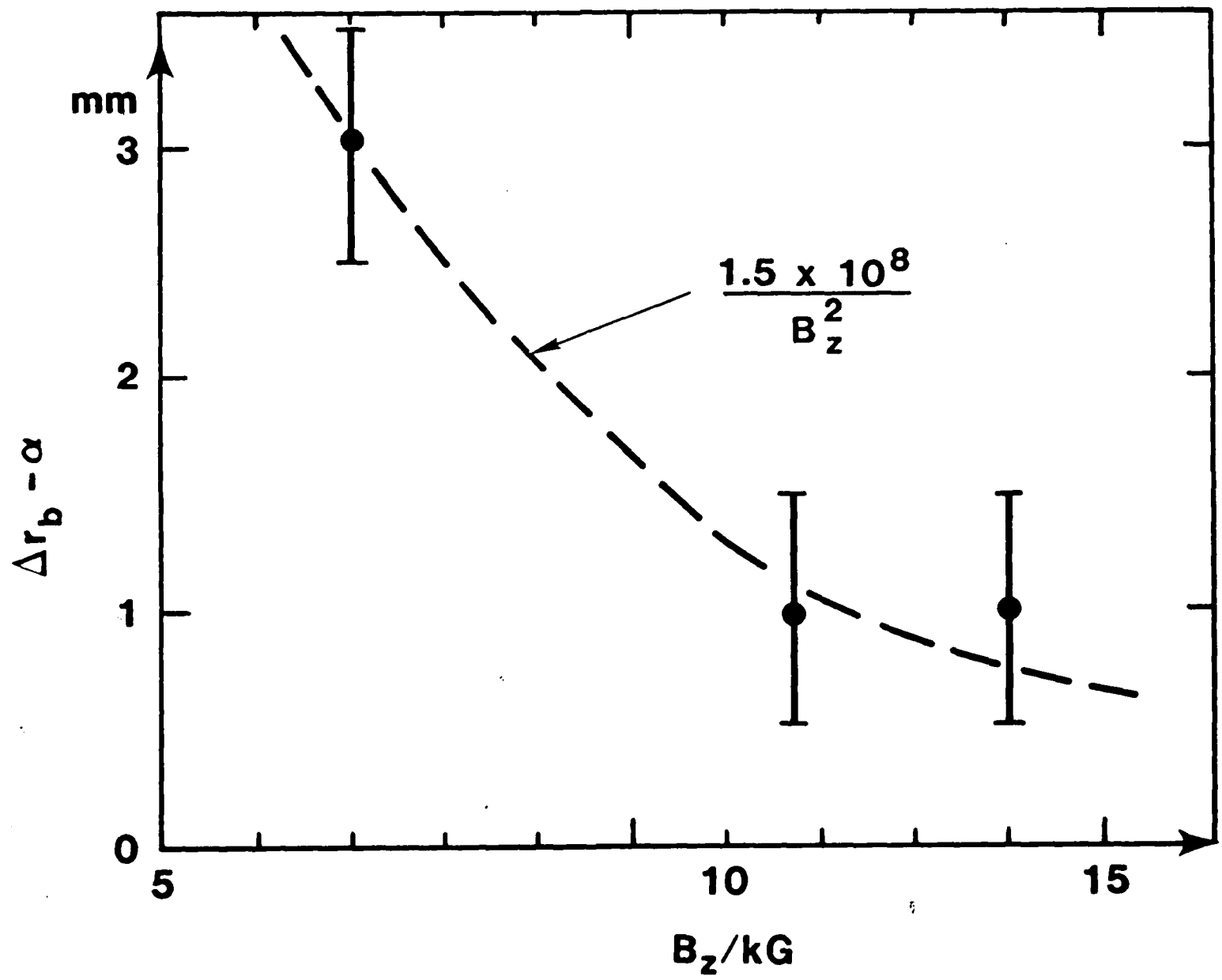

Figure 7. The observed Larmor radii closely follow the quadratic B_z dependence.

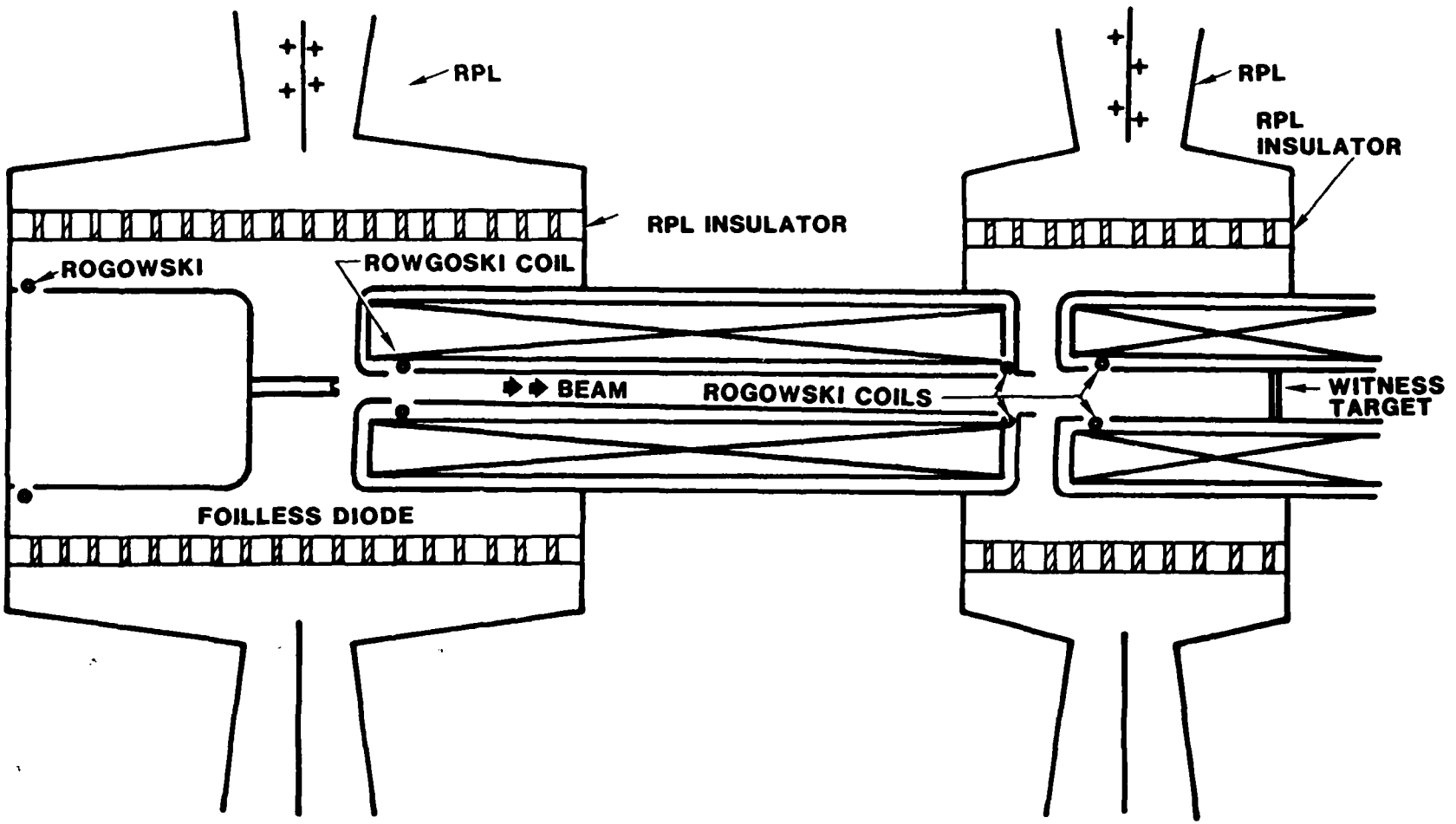

Figure 8. Schematic diagram of the radial oscillation experiment indicating the key components.

experimental set-up. Practically all the hardware used was from RADLAC I. The novelty of this experiment was the balance of the the radial forces at the gap region. Note the different diameter beam pipes before and after the accelerating gap.

Two of the RADLAC Pulse Forming Lines were connected in such a fashion as to provide twice the voltage of a single RPL. This cavity is again an isolated radial Blumlein[11] and has all the advantages of the cylindrical isolated Blumlein of the IBEX accelerator. This configuration provided the accelerating voltage for the injector (2-3 MV). The post accelerating gap used a single RADLAC RPL structure.

The high current beam was supplied by a cold cathode foilless diode injector. An annular beam of outer radius of 1 cm and thickness of 2 mm was emitted from a tubular cathode immersed in the 11 kG guiding field. The beam cross section was measured along its path upstream and downstream of the accelerating gap and in several locations. Brass witness plates were used for these measurements. The experiments were divided into two sets. In the first set, no accelerating voltage was applied to the post accelerating gap, while in the second set both injector and accelerating gap were energized. The Rogowski monitors upstream and downstream of the gap gave practically identical current readings. Because of a slight misalignment between vacuum pipe axis and the guiding magnetic field, the beam envelope was somewhat deformed to an elliptical shape rather than being circular. Figure 9 gives the major (trace a) and minor (trace b) axis of

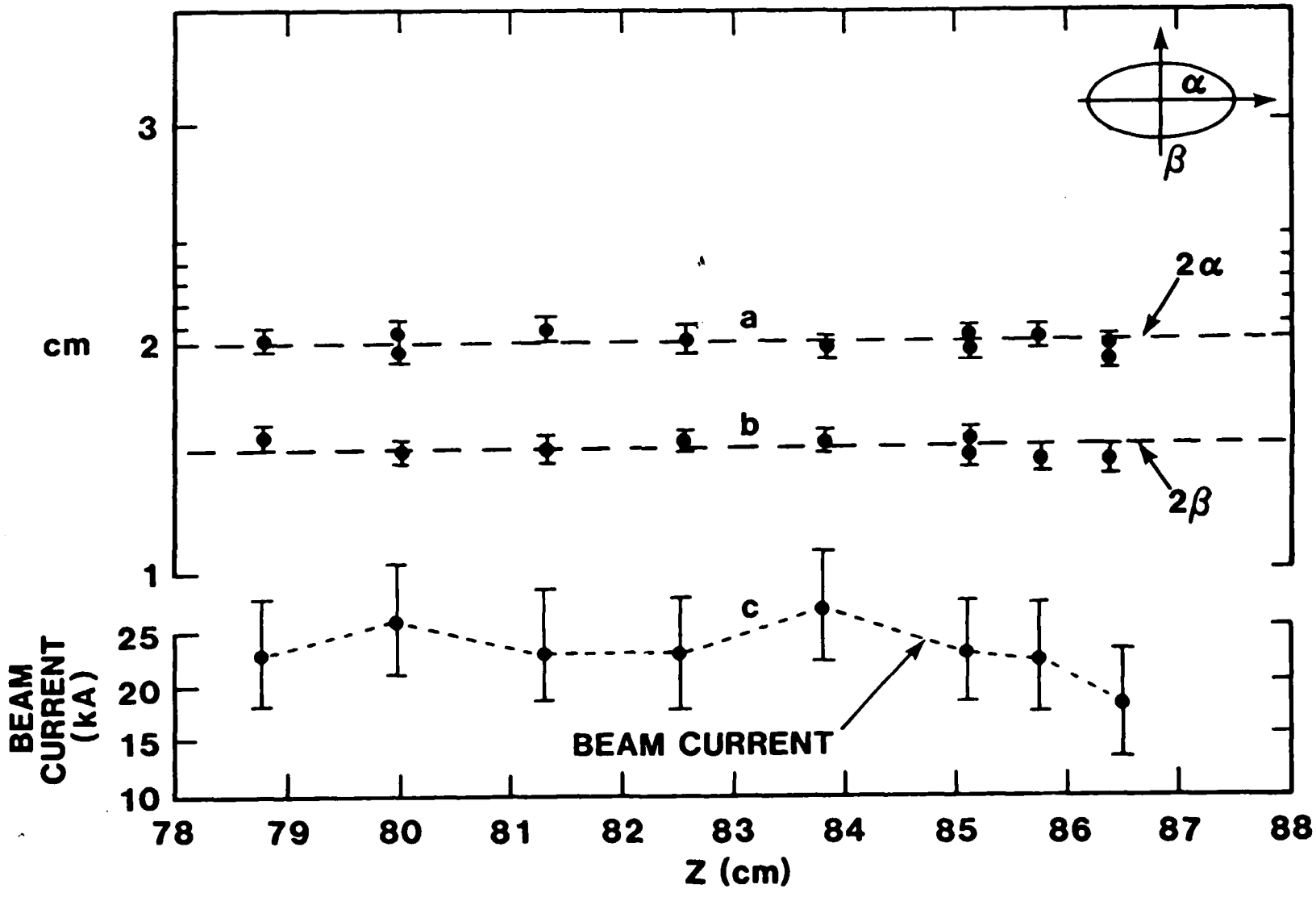

Figure 9. Radial oscillation measurements with the accelerating gap not activated. Trace a gives the major axis (2α) of the beam ellipsis, trace b gives the minor axis (2β) while trace c gives the beam current for every measurement.

the beam ellipsoid. Trace c is the beam current for every envelope measurement. Figure 10 gives the same beam parameters for the second set of experiments. The error bars of 2α and 2β are due to statistical fluctuations in the geometric measurements of the beam imprint on the witness plate. No radial oscillations were observed in either of the sets of experimentation.

IV. Measurements of the Resonant Frequencies ω, Quality Factors Q and Transverse Impedances $Z_\perp$ of Pulsed Transmission Line Cavities.

The coupling of the pulse power system to the electron beam in an induction machine does not involve resonant cavity structures[13] as it does in a conventional rf linear accelerator. The pulse forming line outputs are fed directly to the diode and accelerating gap via transmission lines. Hence, the accelerating cavities should in principle be free of any rf resonances with measurable quality factor Q. Although this may have been true for RADLAC I, as our measurements suggest, it was not the case for the cavities of ETA.

If there exist resonant modes of the accelerating cavities with electromagnetic field patterns such that a transverse magnetic field exists along the beam path, then the passage of the beam pulse can excite those modes. Interaction of the beam pulse with these fields can cause a transverse deflection of the beam. The resulting beam displacements add from cavity to cavity and eventually can lead to a large transverse oscillation and beam losses on the walls of the drift tubes. This instability is called beam break-up

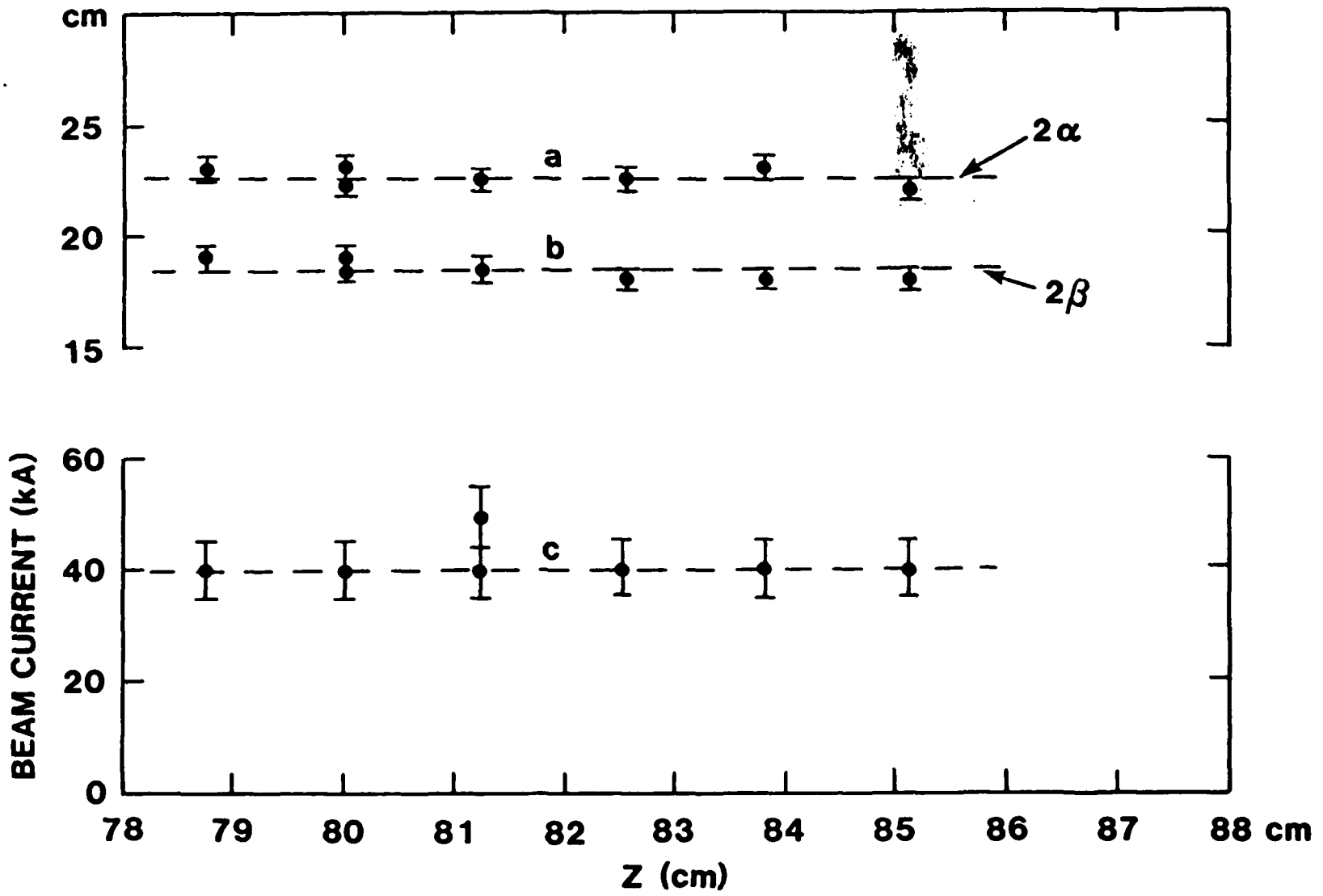

Figure 10. Same beam parameters with the accelerating gap activated to ~ 1 MV. Total accelerating voltage 3 MV.

instability, and it was observed first at SLAC.[5] The magnitude of the beam displacement has been shown to be equal to a power series of the beam accelerator parameters such as pulse width ωt, transverse impedance $Z_\perp$ and beam current, with the order of the series equal to the number of accelerating gaps.[14] The $Z_\perp$ is defined by the following expression:

$$Z_\perp = Q \frac{\left[\int_0^{\ell} B_\perp dz\right]^2 c}{2\omega u} \qquad (1)$$

with ω being the cavity resonant frequency and u the stored energy in the cavity. The integral extends over the accelerating gap of length, ℓ. In order to find the importance of the beam break-up instability for a given cavity design, one must identify the critical eigenfunctions with $B_\perp \neq 0$ on axis and measure the associated Q and the $Z_\perp/Q$.

A typical cavity for a linear accelerator driven by pulse forming lines is shown in Fig. 11. The outer cylindrical wall is composed of metallic and plastic grading rings and serves a double purpose. It acts as a high voltage standoff as well as an interface between the outer dielectric and the vacuum. The inner boundary is defined by the metallic wall of the field shapers. The field shapers are necessary to shorten the accelerating gap and reduce the radial component (E_r) of the accelerating field. In the accelerator assembly, the cavity is surrounded by a liquid dielectric which can be transformer oil, water, or ethylene glycol. These complicated cavity boundaries present a formidable microwave problem for the theoretical and numerical prediction of

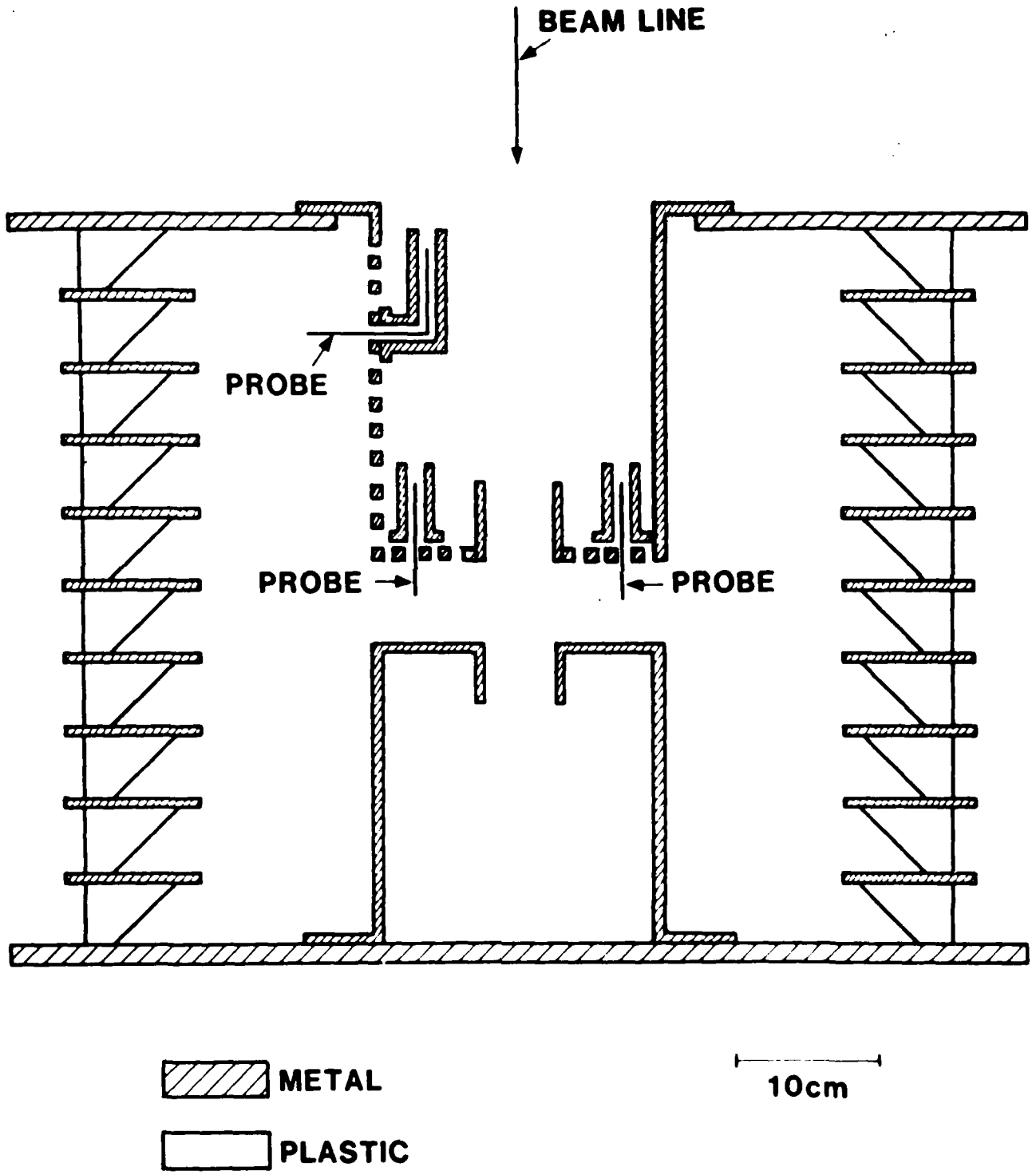

Figure 11. Typical pulsed transmission line cavity. The measuring ports and the probes are also shown.

the various resonant eigenmodes and the corresponding Q and $Z_\perp/Q$ values. Consequently, the direct approach of experimentally identifying the cavity modes and measuring the Q and $Z_\perp/Q$ values was undertaken. The resonant field patterns can be identified by comparison with the relatively simpler modes of a metallic wall pill-box cavity. We are interested only in the TM modes and, in particular, in the TM_{1n} modes since they are the ones that have $B_\perp \neq 0$ along the beam path and are apt to cause beam break-up instabilities.

The mode measurements were made by exciting the cavity with a 1.25 cm long probe. The probe was inserted through openings (Fig. 11) inside the cavity and was rf driven with a sweep oscillator. A similar probe was used to detect the cavity signal which, after passing through a sensor crystal, was amplified and displayed on an oscilloscope as an amplitude versus frequency plot. The scope's horizontal sweep was synchronized with the sweep of the oscillator, such that the horizontal scope scale was directly proportional to the frequency range of the particular frequency sweep of the oscillator. The amplitudes are roughly proportional to the square of the electric fields E_z of the modes, and the peaks correspond to the resonant eigenfrequencies. Figure 12 is a typical photograph of those plots with the resonant modes identified. For the mode identification, only the E_z was measured. The E_z was mapped as a function of the radial (r) and axial (z) position inside the cavity. It is enough to measure only E_z since $B_\perp$ can be directly derived from the expression $B_\perp = \nabla_\perp E_z$. This simple measuring technique completely

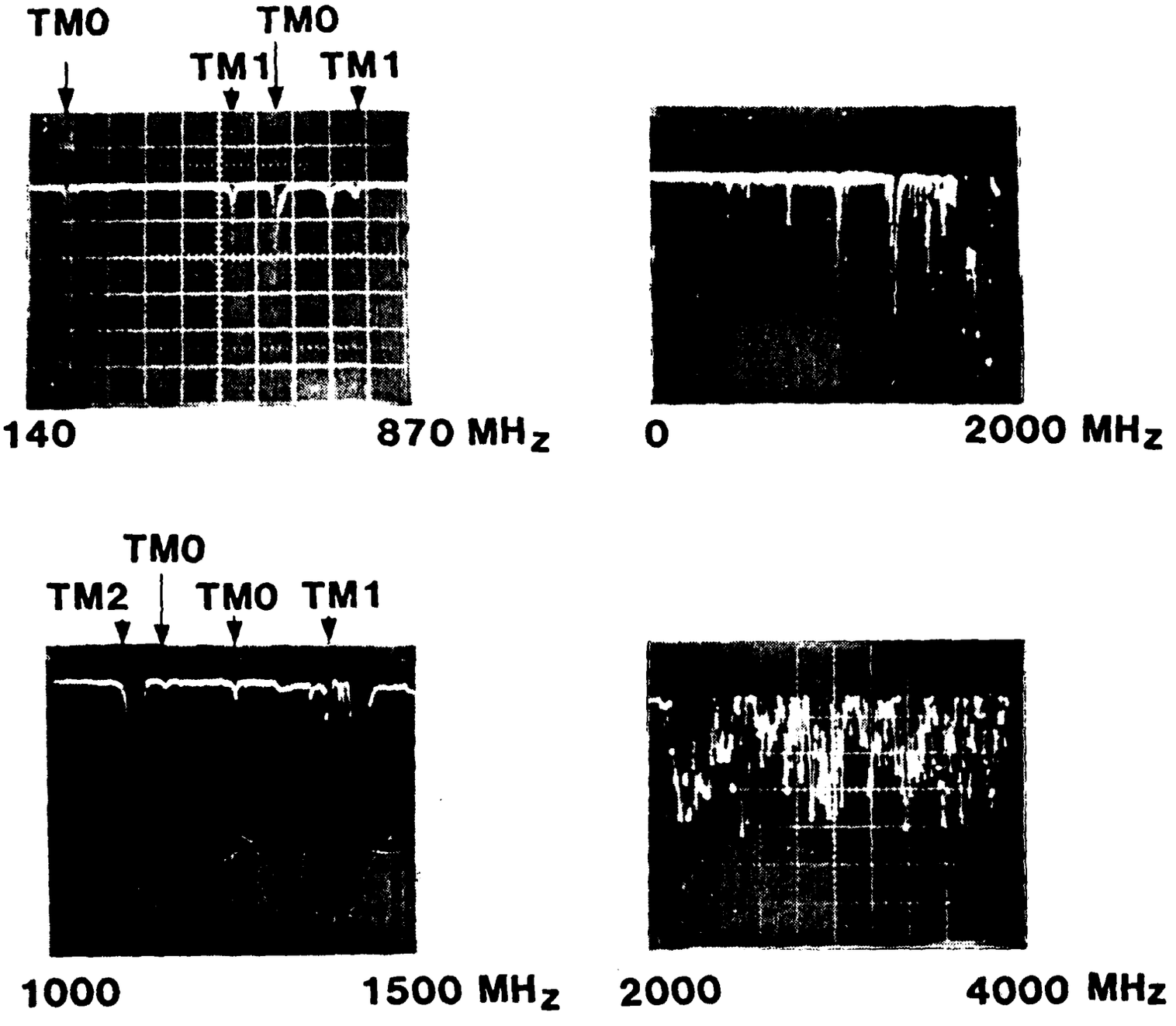

Figure 12. Frequency spectra of copper-lined cavity. The eigenmodes are identified.

identifies the modes of a pill-box cavity. In the case of the "H" shaped cavities studied here, the mode symmetry becomes much more complicated. However, measurements of the E_z in the accelerating gap region should provide unambiguous information about the existence of $B_\perp$ along the beam axis.

The Q of the mode, defined as $\omega/\Delta\omega$, where $\Delta\omega$ is the FWHM of the resonance, was directly obtained from the amplitude versus frequency plots. For the measurements of the $Z_\perp/Q$, the method of Hansen and Post[15,16] was applied. A small metallic cylinder of volume ΔV and radius r was inserted inside the cavity and the frequency shift $\Delta\omega$ for each eigenfrequency was measured. Then from the expression:

$$\frac{Z_\perp}{Q} = \frac{2c^2\mu_0\ell^2}{\left[1 - \left(\frac{r\omega}{2c}\right)^2\right]\omega}\left(\frac{1}{\omega}\ \frac{d\omega}{dV}\right) \quad , \qquad (2)$$

the $Z_\perp/Q$ ratio was estimated.

We first identified the resonant modes. To increase the amplitude of the transmitted signal, we lined the inside wall of the outer shell with a copper sheet. (The copper walls increase the Q of the cavity but do not affect appreciably the eigenmode frequencies). Figure 13 gives the E_z field pattern of the metal walled cavity for one of the TM modes obtained with the E_z probe. Table I summarizes the results of those measurements. As expected, the Q and $Z_\perp/Q$ are relatively high.

In the second stage of the experiment, the copper lining was removed and the cavity was surrounded by water as outer

TABLE I

F (MH_z)	MODE TYPE	Q	Z_1/Q (ohms)
190	TM010	450	--
550	TM110	660	50
620	TM0	170	--
650	TM1	390	70
820	TM1	100	40
1100	TM2	290	--
1150	TM0	760	--
1170	TM0	460	--
1250	TM0	500	--
1380	TM1	1090	25
continuum			

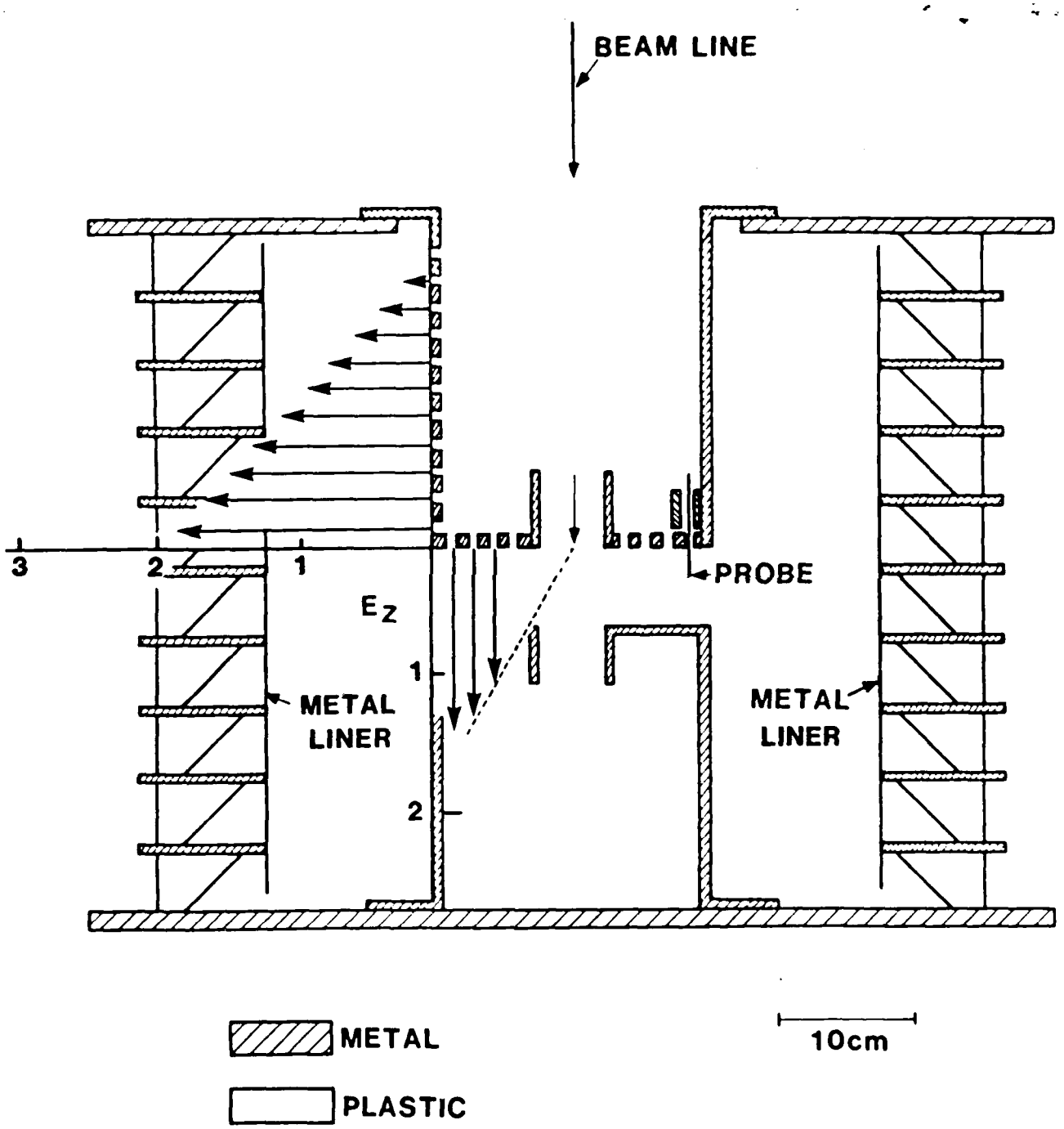

Figure 13. E_z field pattern of the metal walled cavity for one of the TM modes.

dielectric. The plastic grading rings combined with the water made such a lossy environment that we were unable to identify any resonant mode. Increasing the sensitivity of the receiver by a factor of one-hundred did not change the results. No peaks were present at the frequencies of the eigenmodes. From the power output of our sweep oscillator and the sensitivity of our antenna, we believe that values of Q and Z_1/Q of the order of 10 or less could have been observed. Hence, because of the extremely lossy outer cavity walls it would be rather improbable for the beam to excite any transverse resonant modes.

V. Summary

We have developed a very reliable 4 MeV, 40-100 kA electron beam injector. It produces a high quality annular or solid beam of low emittance with no radial oscillations. A new radial force balanced accelerating gap design has been successfully tested and proven to completely eliminate radial oscillations. Finally, an accelerating cavity composed of plastic and metal voltage grading rings immersed in deionized water constitutes such a low Q and Z_1/Q resonator that BBU instabilities become insignificant. The injector, accelerating gap, and cavity presented here can be considered as very promising building blocks for a high-current, high-voltage pulsed, transmission line linear accelerator.

VI. Acknowledgement

The authors thank Ken R. Prestwich for his valuable advice, Juan J. Ramirez and John P. Corley for their assistance with IBEX, and Raymond Brown for his very valuable technical support throughout this project. The advice, support, and continual interest of G. Yonas is greatly appreciated.

This work was supported by the United States Department of Energy under Contract #DE-AC04-76-DP00789 and by the Department of Defense under Contract #N60921-82-WR-W0047.

References

1. N. Christofilos et al., Rev. Sci. Instruments 35, 886 (1964).
2. A. I. Pavlovskii, V. S. Bosamykin, G. I. Kuleshov, A. I. Gerasimov, V. A. Tananakin, and A. P. Klementev, Sov. Phys. Dokl. 70, 441 (1975).
3. A. I. Pavlovskii, V. S. Bosamykin, V. A. Savchenko, A. P. Klementev, K. A. Morunov, V. S. Nikolskiy, A. I. Gerasimov, V. A. Tananakin, V. F. Basmonov, D. I. Zenkov, V. D. Selemir, and A. S. Fedotkin, Dokl. Akad. Nank SSSR 250, 1118 (1980).
4. R. B. Miller, K. R. Prestwich, J. W. Poukey, B. G. Epstein, J. R. Freeman, A. W. Sharpe, W. K. Tucker, and S. L. Shope, J. Appl. Phys. 52, 1184 (1980).
5. W. K. H. Panofsky and M. Bandes, Rev. Sci. Instrum. 39, 206 (1968).
6. R. B. Miller, J. W. Poukey, B. G. Epstein, S. L. Shope, T. C. Genoni, M. Franz, B. B. Godfrey, R. J. Adler, and A. Mondell, IEEE Trans. Nucl. Sci. NS-28, 3343 (1981).
7. J. W. Poukey, S. L. Shope, and R. B. Miller, Proceedings of the 1981 Linear Accelerator Conference, Santa Fe, New Mexico, LA-9234-C, 232 (1981).
8. J. J. Ramirez, J. P. Corley, and M. G. Mazarakis to be published in the "Proceedings of the 5th International Conference on High Power Beams, San Francisco (1983).
9. M. G. Mazarakis, R. B. Miller, S. L. Shope, J. W. Poukey, J. J. Ramirez, C. A. Ekdahl, and R. J. Adler, to be published in the "Proceedings of the 5th International Conference on High Power Beams," San Francisco (1983).

References (Cont'd)

10. R. B. Miller, M. G. Mazarakis, J. W. Poukey, and R. J. Adler, IEEE Trans. Nucl. Sci., NS-30 (4), 2722 (1983).

11. R. B. Miller, K. R. Prestwich, J. W. Poukey, and S. L. Shope, J. Appl. Physics 51 (7), 3506 (1980).

12. T. G. Genoni, M. R. Franz, B. G. Epstein, R. B. Miller, and J. W. Poukey, J. Appl. Phys. 52, 2646 (1981).

13. J. Leiss, IEEE Transactions on Nuclear Science, Vol. NS-26, No. 3, 3870 (1979).

14. V. K. Neil, L. S. Hall, and R. K. Cooper, Particle Accelerators, 9, 213 (1979).

15. W. W. Hansen and R. F. Post, J. Appl. Phys. 19, 1059 (1948).

16. R. J. Adler, T. C. Genoni, and R. B. Miller, IEEE Transactions on Nuclear Sciences, NS-28 (3), 3467 (1981).

Distribution:
UNLIMITED DISTRIBUTION

Director, Defense Advanced Research
Projects Agency
Attn: Lt. Col. Richard L. Gullickson
1400 Wilson Boulevard
Arlington, VA 22209

Commander, Naval Sea Systems Command
Attn: Cdr. William F. Bassett
PMS-405
Washington, DC 20362

Commanding Officer
Naval Research Laboratory
Attn: Dr. J. Robert Greig, 4763
Dr. Martin Lampe, 4790
4555 Overlook Avenue, SW
Washington, DC 20375

Naval Postgraduate School
Attn: Professor R. Andy Smith
Department of Physics, Code 61
Monterey, CA 93940

Department of Nuclear Engineering
University of Michigan
Attn: Professor Ronald M. Gilganbach
Ann Arbor, MI 48109

U. S. Army Ballistic Research Laboratory
DRDAR-BLB
Attn: Dr. Donald Eccleshall
Dr. Anand Prakash
Aberdeen Proving Ground, MD 21005

Air Force Office of Scientific Research
Attn: Capt. Henry L. Pugh, Jr.
Physical and Geophysical Sciences
Bolling Air Force Base
Washington, DC 20332

Air Force Weapons Laboratory
Kirtland Air Force Base
NTYP
Attn: Dr. David C. Straw
Lt. Col. J. Head
Dr. W. Baker
Dr. M. C. Clark
Mr. R. Lemke
Maj. J. Clifford
Albuquerque, NM 87117

Department of Commerce
National Bureau of Standards
Attn: Dr. Samuel Penner
Building 245, B-102
Washington, DC 20234

Lawrence Berkeley Laboratory
Attn: Dr. Edward P. Lee
Building 47, Room 111
1 Cyclotron Road
Berkeley, CA 94720

University of California
Lawrence Livermore National Laboratory
Attn: Dr. Richard J. Briggs, L321
Dr. William Barletta
Dr. D. Prono
P. O. Box 808
Livermore, CA 94550

University of California Irvine
Attn: Dr. Norman Rostoker
Irvine, CA 92717

University of California
Los Alamos National Laboratory
Attn: Dr. Thomas P. Starke, P-942
P. O. Box 1663
Los Alamos, NM 87545

AVCO - Everett Research Laboratory, Inc.
Attn: Dr. Dennis A. Reilly
2385 Revere Beach Parkway
Everett, MA 02149

The Charles Stark Draper Laboratory
Attn: Mr. Edwin A. Olsson
555 Technology Square
Cambridge, MA 02139

TRW, Inc.
Space and Technology Group
Attn: Dr. Edward N. Frazier, R1/2162
One Space Park
Redondo Beach, CA 90278

Austin Research Associates
Attn: Dr. M. Lee Sloan
1901 Rutland Drive
Austin, TX 78758

Directed Technologies, Inc.
Attn: Dr. M. Lee Sloan
1901 Rutland Drive
Austin, TX 78758

GA Technologies, Inc.
Attn: Dr. Richard L. Freeman
P. O. Box 85608
San Diego, CA 92138

Advanced Technology & Mission Analysis
Gould, Inc.
Advanced Systems Division
Attn: Dr. Henry Hidalgo
1235 Jefferson Davis Highway
Suite 1400
Arlington, VA 22202

Hy-Tech Research Corporation
Attn: Dr. Edward J. Yadlowsky
P. O. Box 3422
Radford, VA 24143

Dr. David A. Hammer
109 Orchard Place
Ithaca, NY 14850

JAYCOR
Attn: Dr. Franklin S. Felber
P. O. Box 85154
San Diego, CA 92138

La Jolla Institute
Attn: Dr. Keith Brueckner
P. O. Box 1434
La Jolla, CA 92038

Lockheed Palo Alto Research Laboratory
Attn: Dr. John G. Siambis
3251 Hanover Street
Building 203, Department 52-11
Palo Alto, CA 94304

McDonnel-Douglas Research Laboratory
Attn: Dr. John Leader
P. O. Box 516
St. Louis, MO 63166

Mission Research Corporation
Attn: Dr. Brendan B. Godfrey
Dr. R. Adler
1720 Randolph Road, SE
Albuquerque, NM 87106

Mission Research Corporation
Attn: Dr. N. J. Carron
P. O. Box 719
Santa Barbara, CA 93102

Pulse Sciences, Inc.
Attn: Dr. Sidney D. Putnam
Dr. Ian Smith
14796 Wicks Boulevard
San Leandro, CA 94577

Orlando Technology, Inc.
Attn: Mr.Daniel A. Matuska
P. O. Box 855
Shalimar, FL 32579

Physics International
Attn: Dr. Alan J. Toepfer
2700 Merced Street
San Leandro, CA 94577

The Rand Corporation
Attn: Dr. Simon Kassel
2100 M Street, NW
Washington, DC 20037

Rocketdyne
Attn: Dr. Stanley Gunn
6633 Canoga Avenue
Canoga Park, CA 91304

Science Applications, Inc.
Attn: Dr. Edward P. Cornet
1710 Goodridge Drive
McLean, VA 22102

Science Applications, Inc.
Attn: Dr. W. Reinstra
2340 Alamo, SE - Suite 209
Albuquerque, NM 87106

SRI International
Attn: Dr. Donald J. Eckstrom
PSO-15 Molecular Physics Laboratory
333 Ravenswood Avenue
Meno Park, CA 94025

Texas Tech University
Attn: Professor M. Kristiansen
Department of Electrical Engineering
Lubbock, TX 79409

Titan Systems, Inc.
Attn: Dr. H. L. Buchanan
9191 Towne Centre Drive
Suite 500
San Diego, CA 92122

University of New Mexico
Department of Chemical and
Nuclear Engineering
Attn: Professor Stanley Humphries
Albuquerque, NM 87131

University of Texas
Austin Institute for Fusion Studies
RLM 11.218
Attn: Dr. Marshall N. Rosenbluth
Austin, TX 78712

Naval Surface Weapons Center
Attn: Dr. C. M. Huddleston, R401
Dr. Moon H. Cha, R41
Dr. Han S. Uhm, R41
Dr. Eugene E. Nolting, F53
White Oak, Silver Spring, MD 20910

U. S. Military Academy
Science Research Laboratory
Attn: Lt. Col. T. C. Genoni
West Point, NY 10996

U. S. Army Ballistic Missile Defense
Advanced Technology Center
Attn: Mr. M. C. Hawie
P. O. Box 1500
Huntsville, AL 35807

Office of High Energy and Nuclear Physics
Office of Energy Research
U. S. Department of Energy
Attn: Dr. J. E. Leiss
Washington, DC 20545

300 R. L. Hagengruber
1000 W. F. Brinkman
1200 J. P. VanDevender
1220 M. Cowan
1230 J. E. Powell
1240 K. R. Prestwich
1241 J. R. Freeman
1241 R. Coats
1241 C. L. Olson
1241 J. W. Poukey
1241 J. P. Quintenz

1241	D. B. Seidel
1241	J. A. Swegle
1241	J. S. Wagner
1244	R. A. Gerber
1245	D. E. Hasti
1248	M. T. Buttram
1250	T. H. Martin
1260	J. P. VanDevender (Acting)
1270	R. B. Miller
1271	M. J. Clauser
1271	J. E. Brandenburg
1271	T. W. Hussey
1271	R. J. Lipinski
1271	C. J. MacCallum
1271	E. J. McGuire
1271	J. M. Peek
1272	C. A. Ekdahl
1272	P. D. Coleman
1272	C. A. Frost
1272	D. J. Johnson
1272	G. T. Leifeste
1272	T. R. Lockner
1272	M. G. Mazarakis
1272	G. S. Mills
1273	M. K. Matzen
1273	R. J. Dukart
1273	W. W. Hsing
1273	M. A. Palmer
1273	R. B. Spielman
3141	C. M. Ostrander (5)
3151	W. L. Garner (3)
3154-3	C. H. Dalin, for DOE/TIC (25)
8424	M. A. Pound

END

FILMED

8-85

DTIC